Alpha-Particle Reaction Cross Sections at 40 MeV

G. IGO AND B. D. WILKINS
Lawrence Radiation Laboratory, University of California, Berkeley, California
(Received 31 January 1963; revised manuscript received 29 April 1963)

We have measured the nonelastic cross section σ_R for 40-MeV alpha particle for 19 target elements ranging in atomic weight A between 9 and 232. The results have been compared with the predictions of the optical model σ_I. The ratio σ_R/σ_I deviates from unity in a systematic fashion being less than 1 for the lightest elements and greater than 1 for the heaviest. Superimposed on this trend, σ_R/σ_I dips by 18% for elements where the nuclear charge is near 28. A similar effect had been noted earlier in proton-reaction cross-section data but not in deuteron-reaction cross-section data.

WE have measured the reaction cross section σ_R for 40-MeV alpha particles, and we compare it with the prediction σ_I of the optical-model potential for alpha particles.[1,2] The ratio σ_R/σ_I plotted against $A^{2/3}$ (A, the atomic number) deviates from unity in a systematic fashion. A straight line with a slope of 5.5×10^{-3} fits the data in Fig. 1. Superimposed on this trend, σ_R/σ_I dips by 18% near $A=28$ protons as was also noted in the 10-MeV proton measurements.[3]

The experimental apparatus used in the reaction cross-section measurements (see Fig. 2) has been described in detail elsewhere[4] and will not be discussed here except where parameters of the experiment have been altered because of the change in the projectile. A beam particle is defined by a coincidence event between counters 1, 2, 3, and 4 of the kind $1\,\bar{2}\,3\,\bar{4}$, where a bar denotes a counter in anticoincidence. In what follows we understand that the intensity I_0 represents the frequency of events of this kind, i.e., $I_0=1\,\bar{2}\,3\,\bar{4}$. In the attenuation technique utilized here the quantity I_0-I is measured by placing counter 5 (see Fig. 2) in anticoincidence, i.e., $I_0-I=1\,\bar{2}\,3\,\bar{4}\,\bar{5}$.

Absorption of the alpha particles occurs more frequently in the degrader (see Fig. 2), since it is several times as thick as the targets. This contribution had to be subtracted. This is done by removing the target and placing a "dummy" target in the beam ahead of the scattering foil of such a thickness that the beam energy incident on the degrader foil is the same, and the numbers of $i_0(=1\,\bar{2}\,3\,\bar{4})$ and $i_0-i(=1\,\bar{2}\,3\,\bar{4}\,\bar{5})$ events are measured.

Since elastic and inelastic scattering cannot, in general, be neglected, counter 5 must subtend an angle θ large enough so that the elastic scattering $\int_{\theta_5}^{\pi}\sigma_{\rm el}(\theta)d\Omega$ outside the angle θ_5 [where $\sigma_{\rm el}(\theta)$ is the differential elastic-scattering cross section], is not so large that the uncertainty in this quantity limits the accuracy of the measurement. Of course, θ_5 is made as small as is possible to reduce the inelastic contribution

$$\sum_{i=0}^{N}\int_0^{\theta}\sigma_i(\theta)d\Omega,$$

where $\sigma_i(\theta)$ is the differential inelastic cross section for the excitation of the ith level of the target element, and the sum extends from the ground state up to the Nth state. Higher lying states are excluded by the energy resolution afforded by the degrader. By $\sigma_0(\theta)$ we mean the compound elastic differential cross section.

When a "target-in" measurement (I_0, I_0-I) and a "dummy-in" measurement (i_0, i_0-i) are made, the energy of the proton incident on the degrader is the same order that absorptive effects in the degrader will be exactly compensated for. However, this has the serious effect of changing the energy that the alpha particles have when they are incident on counter 3 in the two configurations. Counter 4 (see Fig. 2) in anticoincidence greatly reduces the effect of scattering out in counter 3. However, the number of alpha particles scattered out at larger angles than the angle θ_4 subtended by counter 4 is still appreciable. The quantity

$$\int_{\theta_4}^{\pi}\left[\sigma_{\rm SE}(\theta)+\sum_{i=0}^{1}\sigma_i(\theta)\right]d\Omega=\eta$$

[$\sigma_{\rm SE}(\theta)$ is the differential cross section for shape elastic scattering] was, therefore, measured. In order to do so, the degrader was removed from counter 5, the target was removed, and the quantity $(i_0-i)/i_0$ was measured

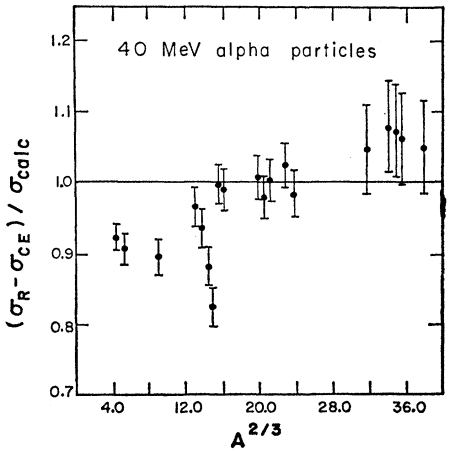

FIG. 1. The ratio of the nonelastic cross section for 40-MeV alpha particles $\sigma_R-\sigma_{CE}$ and the corresponding theoretical value σ_I versus the two-thirds power of A.

[1] G. Igo, Phys. Rev. Letters **1**, 72 (1958); Phys. Rev. **115**, 1665 (1959).
[2] J. R. Huizenga and G. Igo, Nucl. Phys. **29**, 462 (1962).
[3] G. Igo and B. D. Wilkins, Phys. Letters **2**, 342 (1962).
[4] B. D. Wilkins and G. Igo, Phys. Rev. **129**, 2198 (1963).

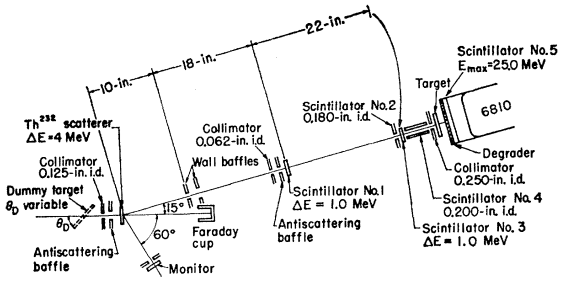

FIG. 2. Schematic diagram of the experimental apparatus.

as a function of beam energy. The beam energy was reduced by the insertion of foils before the lead scattering foil. Anticoincidence events obtained in this configuration are due to reactions or elastic scattering in counter 3. A quantity $\eta_3=(\eta_t-\eta_d)$ is defined, where η_t and η_d are the values of η at different energies for two configurations, i.e., target-in and dummy-in. The scattering-out correction η_3 due to counter-3 events discussed above is obtained and applied to the measurement. The experimental quantities I_0, I_0-I, i_0, i_0-i, and η_3 are related to the quantity of interest σ_R by the equation

$$\sigma-\eta_3\frac{n'x'}{nx}=\left[\left(\frac{I_0-I}{I_0nx}\right)-\left(\frac{i_0-i}{i_0nx}\right)-\eta_3\frac{n'x'}{nx}\right]$$
$$=\sigma_R+\int_{\theta_5}^{\pi}\sigma_{\mathrm{SE}}(\theta)d\Omega-\int_0^{\theta_5}\sum_{i=0}^{N}\sigma_i(\theta)d\Omega,$$

where n is the target density; x, the target thickness; n', the counter-3 density; and x', the counter-3 thickness. The quantity θ_5 is the angle subtended by counter 5. Combining the results of this measurement and the elastic scattering data, we obtain the quantity

$$\left[\left(\frac{I_0-I}{I_0nx}\right)-\left(\frac{i_0-i}{i_0nx}\right)-\eta_3\frac{n'x'}{nx}\right]-\int_{\theta_5}^{\pi}[\sigma_{\mathrm{SE}}(\theta)+\sigma_0(\theta)]d\Omega$$
$$=\sigma_R-\int_0^{\pi}\sigma_0(\theta)d\Omega-\int_0^{\theta_5}\sum_{i=1}^{N}\sigma_i(\theta)d\Omega$$
$$=\sigma_R-\sigma_{\mathrm{CE}}-\int_0^{\theta_5}\sum_{i=1}^{N}\sigma_i(\theta)d\Omega,$$

where σ_{CE} is the compound elastic cross section, and σ_R is the reaction cross section. The raw cross section σ, obtained from the target-in and target-out measurements, is listed in Table I. The three principal corrections which must be made to σ are also listed. Fortunately, the counter-3 scattering-out correction $\eta_3(n'x'/nx)$ can be measured quite accurately.[3] With regard to the second correction

$$\sigma_{\mathrm{el}}=\int_{\theta_5}^{\pi}[\sigma_{\mathrm{SE}}(\theta)+\sigma_0(\theta)]d\Omega,$$

due to those elastic events where scattering occurs outside of the solid angle subtended by counter 5, the angle θ_5 was set as follows: 28.7° for light and intermediate elements, and for elements heavier than tin, at 43.0°. The third correction

$$\int_0^{\theta_5}\sum_{i=1}^{N}\sigma_i(\theta)d\Omega=\sigma_{\mathrm{in}}$$

is comprised from part of the inelastic and reaction events scattered into the solid angle subtended by the stopping counter. In order to facilitate the separation of elastic events from the inelastic and reaction events, a degrader foil is placed between the target and counter 5. The thickness of the degrader foil was adjusted so that 25-MeV alpha particles are stopped by it.

The correction σ_{in} is due to several sources. The first is the correction due to (α,α') direct-interaction events[5–9] (evaporation-spectrum alpha particles will stop in the absorber). The correction due to (α,p) events has been obtained using the Nuclear Monte Carlo Evaporation Model (NMCEM).[10] Experimental data,[11–15] fit with

TABLE I. The raw cross section σ, the counter-3 scattering-out correction η_3, the inelastic and reaction scattering correction σ_{in} (Ref. 5–17), the elastic scattering correction σ_{el}, (Refs. 7, 8, 18–20), and the nonelastic cross section $\sigma_R-\sigma_{\mathrm{CE}}$.

Element	σ (mb)	$-\eta_3(n'x'/nx)$ (mb)	σ_{in} (mb)	σ_{el} (mb)	$\sigma_R-\sigma_{\mathrm{CE}}$ (mb)
Be	789±7	9±4	36±7	51±3	783±11
C	894±12	12±6	60±9	65±3	901±16
Al	1105±17	23±10	54±8	41±2	1141±21
Ti	1422±30	32±18	77±12	31±5	1500±37
V	1397±32	43±18	80±12	31±5	1480±39
Fe	1363±34	36±20	68±12	31±5	1436±42
Ni	1271±28	40±18	79±15	36±2	1354±37
Cu	1526±36	42±19	128±26	50±3	1646±48
Zn	1511±37	42±19	129±26	48±3	1639±49
Zr	1753±48	45±32	97±23	124±7	1771±63
Nb	1704±52	53±27	105±24	134±7	1728±64
Mo	1792±65	47±34	103±24	160±10	1782±78
Ag	1881±52	61±27	99±25	195±10	1846±64
Sn	1858±65	59±34	97±25	246±13	1768±78
Ta	1846±83	79±44	97±25	136±7	1886±97
Au	1931±63	88±39	100±25	200±10	1919±79
Pb	1953±62	89±42	100±30	250±13	1892±82
Bi	1923±87	100±46	100±30	270±20	1853±105
Th	1973±84	92±51	100±30	404±20	1761±105

[5] R. Beurtey, R. Catillon, R. Chauminades, M. Crut, H. Faraggi, A. Papineau, J. Saudinos', and J. Thirion, Compt. Rend. **252**, 1756 (1961).
[6] J. Van Heerden and D. J. Prowse, Nucl. Phys. **15**, 356 (1960).
[7] R. G. Summers-Gill, Phys. Rev. **109**, 1591 (1958).
[8] J. L. Yntema, B. Zeidman, and B. J. Ray, Phys. Rev. **117**, 801 (1960).
[9] D. K. McDaniels, J. S. Blair, S. W. Chen, and G. W. Farwell, Nucl. Phys. **17**, 614 (1960).
[10] I. Dostrovsky, Z. Fraenkel, and G. Friedlander, Phys. Rev. **116**, 683 (1959).
[11] N. T. Porile, Phys. Rev. **115**, 939 (1959).
[12] R. Vandenbosch, T. D. Thomas, S. E. Vandenbosch, R. A. Glass, and G. T. Seaborg, Phys. Rev. **111**, 1358 (1958).
[13] B. Foreman, Lawrence Radiation Laboratory Report UCRL-8223, 1958 (unpublished).
[14] N. O. Lassen and V. A. Sidorov, Nucl. Phys. **19**, 579 (1960).
[15] N. T. Porile and D. L. Morrison, Phys. Rev. **116**, 1193 (1959).

this model, were used to fix the parameters of the model. The predictions of the model for (α,p) cross sections were then calculated. Instead of using a parameter for shell corrections fit to each element, as was done in Ref. 10, Cameron's empirical shell correction[16] was used. This gave consistently good fits to the experimental data throughout the Periodic Table. The (α,d) and (α,t) corrections were also calculated and found to be small (about 5 mb). The (α,He^3) reaction did not contribute because of the large Q value associated with this reaction. The NMCEM does not treat the direct interaction (α,p) events properly. To compensate for this, the NMCEM calculations were adjusted to fit the average of the peaked forward, direct interaction distributions[17] determined experimentally. It is, therefore, possible that we have underestimated the contribution of the direct interaction (α,p) events, especially in the light elements where σ_R/σ_I is <1 (see Fig. 1). Unfortunately, no measurements at the extreme forward angles corresponding to the solid angle intercepted by counter 5 exists to check on this. The values predicted by NMCEM, when normalized to the measured σ_R, fit the excitation function peaks within 1 MeV, and the absolute magnitude of the excitation function data was usually fit within 20%.

The elastic scattering correction σ_{el} has been estimated from the literature.[7,8,18–20] The elastic scattering data are the sum of shape elastic scattering σ_{SE} and compound elastic scattering σ_{CE}. The latter is not included in the measured quantity in these experiments. The final result $\sigma_R-\sigma_{CE}$, where σ_R is the total reaction cross section, is listed in the last column of Table I. The results for $(\sigma_R-\sigma_{CE})/\sigma_I$ are also shown in Fig. 1 where the deviation from unity can be seen. The most prominent features are the agreement with unity for $A^{2/3}\geq 16$, the dip near 28 proton nuclei, and a 10% deviation for light elements. It has been emphasized above that some of this deviation could be due to an underestimate of the (α,p) direct interaction cross sections. The data can be fit by a straight line with slope of 5.5×10^{-3} on this plot versus $A^{2/3}$ if the dip near 28-proton nuclei is neglected. It also should be noticed that we plot $(\sigma_R-\sigma_{CE})/\sigma_I$ versus $A^{2/3}$. However, at 40 MeV, σ_{CE} is expected to be small, and we do not believe that the dip is due to a resonance in σ_{CE}. Instead, it probably reflects the decrease in the cross-sectional area of nuclei in this region. The same effect was seen in $\sigma_R-\sigma_{CE}$ for 10-MeV protons,[3,4] but not seen in the 22.4-MeV deuteron-reaction cross-section data.[21]

[16] A. G. W. Cameron, CRP-690, 1957 (unpublished).
[17] R. M. Eisberg, G. Igo, and H. E. Wegner, Phys. Rev. **100**, 1309 (1955).
[18] A. I. Yavin and G. W. Farwell, Nucl. Phys. **12**, 1 (1959).
[19] G. Igo, H. E. Wegner, and R. M. Eisberg, Phys. Rev. **101**, 1508 (1956).
[20] H. E. Wegner, R. M. Eisberg, and G. Igo, Phys. Rev. **99**, 825 (1955).
[21] B. D. Wilkins and G. Igo, Phys. Rev. Letters (to be published).